

MOL #76067

Title: Transient Receptor Potential Vanilloid-1 (TRPV1) Is a Mediator of Lung Toxicity for Coal Fly Ash Particulate Material

Authors: Cassandra E. Deering-Rice, Mark E. Johansen, Jessica K. Roberts, Karen C. Thomas, Erin G. Romero, Jeewoo Lee, Garold S. Yost, John M. Veranth, and Christopher A. Reilly

Affiliations:

Department of Pharmacology and Toxicology, University of Utah, 30 S. 2000 E., Room 201 Skaggs Hall, Salt Lake City, UT 84112, USA. C.E.D-R., M.E.J., J.K.R., K.C.T., E.G.R., G.S.Y., J.M.V., and C.A.R.

College of Pharmacy, Seoul National University, Shinlim-Dong, Kwanak-Ku, Seoul 151-742, Korea. J.L.

Running Title: Activation of TRPV1 by Particulate Material

Corresponding Author:

Dr. Christopher A. Reilly, Ph.D.
University of Utah
Department of Pharmacology and Toxicology
30 South 2000 East, 201 Skaggs Hall
Salt Lake City, UT 84112.
Phone: (801) 581-5236
FAX: (801) 585-3945
Email: Chris.Reilly@pharm.utah.edu

Number of text pages:	34
Number of Tables:	0
Number of Figures:	7
References:	50
Number of words in Abstract:	233
Number of words in Introduction:	556
Number of words in Discussion:	1238

Non-Standard Abbreviations: PM, particulate matter; TRPA1, transient receptor potential ankyrin-1; TRPM8, transient receptor potential melastatin-8; TRPC4 α , transient receptor potential canonical-4, alpha variant; TRPV1, transient receptor potential vanilloid-1; TRPV2, transient receptor potential vanilloid-2; TRPV3, transient receptor potential vanilloid-3; TRPV4, transient receptor potential vanilloid-4; AITC, allyl isothiocyanate; LJO-328, (*N*-(4-*tert*-butylbenzyl)-*N'*-(1-[3-fluoro-4-(methylsulfonylamino)phenyl]ethyl)thiourea); EGTA, ethylene glycol tetraacetic acid; CFA1, power plant coal fly ash; CFA2, laboratory-generated-coal fly ash; DEP, diesel exhaust particles; MUS, Min-U-Sil 5 μ M, crystalline silica; DD, desert dust particulate; nSiO₂, nano silica; HEK-293, human embryonic kidney-293 cells; HEK-293-OE cells; HEK cells engineered to over-express a TRP channel; BEAS-2B, human bronchial epithelial cells; NHBE, normal human bronchial epithelial cells; LHC-9, Lechner and LaVeck media; BEGM, bronchial epithelial growth medium.

Abstract:

Environmental particulate pollutants (PM) adversely affect human health, but the molecular basis is poorly understood. The ion channel TRPV1 has been implicated as a sensor for environmental PM and a mediator of adverse events in the respiratory tract. The objectives of this study were: to determine if TRPV1 can distinguish chemically and physically unique PM that represent important sources of air pollution; to elucidate the molecular basis of TRPV1 activation by PM; and to ascertain the contributions of TRPV1 to human lung cell and mouse lung tissue responses exposed to an insoluble PM agonist, coal fly ash (CFA1). The major findings of this study are: TRPV1 is activated by some, but not all of the prototype PM materials evaluated, with responses to CFA1 > diesel exhaust PM > crystalline silica; TRPM8 is also robustly activated by CFA1, while other TRP channels expressed by airway sensory neurons and lung epithelial cells that may also be activated by CFA1, including TRPA1, C4 α , M2, V2, V3, or V4, were either slightly (TRPA1) or not activated by CFA1; activation of TRPV1 by CFA1 occurs via cell surface interactions between the solid components of CFA1 and specific amino acid residues of TRPV1 that are localized in the putative pore-loop region; and activation of TRPV1 by CFA1 is not exclusive in mouse lungs, but represents a pathway by which CFA1 impacts the expression of selected genes in lung epithelial cells and airway tissue.

Introduction:

Environmental particulate air pollution (PM) is a heterogeneous mixture of geometrically and chemically diverse solids with adsorbed chemicals produced mainly by suspension of geological and road materials, combustion of solid fuels, and secondary atmospheric chemical reactions (Lighty et al., 2000). PM in the size range of 2.5-10 μm constitute the majority of urban air pollution mass, and these materials deposit throughout the respiratory tract where they can produce serious adverse effects including tissue damage and local and systemic changes in physiology. Even slight ($10 \mu\text{g}/\text{m}^3$) increases in ambient PM can trigger airway inflammation and injury, reflected clinically as airway irritation and cough, and epidemiologically, as increased rates of hospitalization and premature death, largely attributable to acute cardiopulmonary dysfunction (Bernstein et al., 2004; Ward and Ayres, 2004). Not all people are similarly affected by PM. Developing fetuses (Glinianaia et al., 2004), infants and children (Ward and Ayres, 2004; Chow et al., 2006), elderly (Pope et al., 2008), and individuals with pre-existing respiratory or heart disease (Bernstein et al., 2004; Pope et al., 2008) are significantly more sensitive. However, the molecular basis for adverse responses to PM is still unclear.

Transient Receptor Potential Vanilloid-1 (TRPV1), a calcium ion channel activated by the botanical irritant capsaicin, endovanilloids, H^+ , organic acids, and temperature $>42^\circ\text{C}$ (Jia et al., 2005; Bessac and Jordt, 2008), has been implicated as a potential mediator of cellular responses to PM in the lung, since inhibition of TRPV1 substantially reduces some of the acute adverse outcomes associated with PM inhalation exposure (Veronesi et al., 1999a; Veronesi et al., 1999b; Oortgiesen et al., 2000; Agopyan et al., 2003a; Agopyan et al., 2003b; Wong et al., 2003; Ghelfi et al., 2008). TRPV1 is also expressed by epithelial cells of the major airways and alveoli, and activation of TRPV1 in these cells by PM, has been correlated with the production of

immunomodulatory cytokines and chemokines including IL-6, IL-8 and TNF α , and cell death *in vitro* (Veronesi et al., 1999a; Veronesi et al., 1999b; Oortgiesen et al., 2000; Agopyan et al., 2003a; Agopyan et al., 2003b; Reilly et al., 2003; Reilly et al., 2005; Thomas et al., 2011).

Many acute adverse responses to concentrated urban PM have also been associated with activation of capsaicin-sensitive (i.e., TRPV1 positive) bronchopulmonary C-fiber neurons that initiate pulmonary reflex responses including cough and reduced compliance, as well as edema. These neurons release substance P (SP) and neurokinin A (NKA), among other substances, that promote abrupt changes in cardiopulmonary function, lung-vascular fluid barrier function, and stimulate pro-inflammatory mediator production by non-neuronal cells (Reilly, 2010).

While existing literature strongly supports a role for TRPV1 as a mediator of several major adverse effects of PM in the lung and on respiratory function, it is not clear how PM interacts with TRPV1 to elicit such responses, whether TRPV1 is a selective or indiscriminant sensor of environmental PM (i.e., do other TRP or calcium channels also detect PM and promote toxicity), or if activation of TRPV1 is directly coupled with processes that influence deleterious changes in airway homeostasis. The objectives of this study were to determine if TRPV1 can distinguish chemically and physically unique forms of PM, to elucidate the molecular basis of TRPV1 activation by such PM, and to ascertain the contributions of TRPV1 to potentially deleterious lung cell and tissue responses elicited by treatment with a moderately selective PM agonist.

Materials and Methods:

Chemicals and Reagents: *n*-Vanillylnonanamide (nonivamide; a capsaicin analogue), (-)-menthol, icilin, allyl isothiocyanate (AITC), hydrogen peroxide (H₂O₂; 30%), carvacrol, Δ^9 -tetrahydrocannabinol (THC), GSK1016790A, carbachol (carbamoyl choline), ionomycin,

EGTA, and ruthenium red were purchased from Sigma-Aldrich (St. Louis, MO) and LJO-328 (*N*-(4-*tert*-butylbenzyl)-*N'*-(1-[3-fluoro-4-(methylsulfonylamino)phenyl]ethyl)thiourea) was synthesized by Dr. Jeewoo Lee. The structure of LJO-328 is also available in the following reference (Reilly et al., 2005). H₂O₂ concentrations were determined spectrophotometrically using the extinction coefficient $\epsilon_{240}=39.4 \text{ M}^{-1}\text{cm}^{-1}$. PCR primers were synthesized by the University of Utah DNA synthesis core facility.

Cells and Cell Culture: Immortalized human bronchial epithelial cells (BEAS-2B) were purchased from American Type Culture Collection (Manassas, VA). TRPV1 over-expressing BEAS-2B (TRPV1-OE) cells were generated as previously described (Reilly et al., 2003). BEAS-2B and TRPV1-OE cells were cultured in LHC-9 media (Invitrogen). Primary normal human bronchial epithelial cells (NHBE), were purchased from Lonza (Walkersville, MD), and were cultured in BEGM media. Culture flasks for all three cell types were pre-coated with LHC basal media fortified with 30 $\mu\text{g}/\text{mL}$ collagen, 10 $\mu\text{g}/\text{mL}$ fibronectin, and 10 $\mu\text{g}/\text{mL}$ BSA. Cells were maintained between 30 and 90% maximum density in a humidified incubator at 37°C with a 5% CO₂:95% air atmosphere, and were sub-cultured using trypsin.

Particulate Materials (PM): Six chemically and physically different combustion-derived, soil-derived, and manufactured PM, representative of PM that are found in ambient air, were selected as a test set for identifying TRPV1 agonists, based on their environmental relevance, and variable effects on lung cells and/or tissue, as described by our group and others (Veronesi et al., 1999a; Veronesi et al., 1999b; Agopyan et al., 2003a; Agopyan et al., 2003b; Veranth et al., 2004; Smith et al., 2006; Veranth et al., 2006; Veranth et al., 2008; Deering-Rice et al., 2011). CFA1 is a size-fractionated sample of coal fly ash collected from a power plant in Utah. This material is derived from combustion of low-sulfur bituminous coal and represents

“real-world” coal ash emitted directly from combustion of coal and/or from physical breakdown of CFA-fortified pavement and cement. CFA1 is principally insoluble mineral oxides and salts of (% by weight) silicon (12.4%), calcium (5.6%), aluminum (4.9%), and iron (4.2%), partially as sulfates (4%), with ~3% elemental carbon and ~1% unspecified organic carbon (Smith et al., 2006), presumably PAHs as described for other CFA samples (Cao et al., 2001). CFA2 (20% elemental carbon) was generated in a laboratory-scale research furnace by combustion of coal under low air conditions. The mineral ash component of CFA2 is similar to CFA1 in shape and size, but CFA2 also contains agglomerates of submicron soot particles and irregular particles of unburned coal char. Diesel exhaust PM (DEP) was collected from scraping the tailpipe of an in-service 2004 Ford F350 “black smoker” truck and represents a high soot-content PM from a poorly functioning, but environmentally relevant diesel engine. The DEP sample consists of loose agglomerates of submicron primary particles and is comparable to NIST SRM 2975 with respect to its ability to activate TRPA1 and other TRP channels (Deering-Rice et al., 2011). Crystalline silica (MUS) is Min-U-Sil 5 (5 μm) (US Silica, Mill Creek, OK). MUS represents silica PM produced by mechanical grinding of mineral material and a redox active PM. Details on the elemental composition of CFA1 and scanning electron micrographs of CFA1, CFA2, DEP, and MUS can be found in Deering-Rice *et al.* (Deering-Rice et al., 2011) and Smith *et al.* (Smith et al., 2006). Desert dust (DD) is a calcium-rich dust that was collected from an arid and sparsely vegetated area south of the salt flats in Tooele County, UT (Veranth et al., 2004). DD PM was size fractionated to be (2.5-10 μm) using a rotary tumbler connected to an Anderson cascade impactor. Details on DD composition can be found in the following reference (Veranth et al., 2004) and nano SiO₂ (nSiO₂) (10 nm, spherical) is a manufactured amorphous material (Nanostructured and Amorphous Materials, Los Alamos NM).

TRP Channel Cloning, TRP Channel Over-expression, and Site-Directed Mutagenesis:

Human TRPA1, C4 α , M8, the N-terminal truncated TRPM8 Δ 1-801 variant, V1, V2, V3, and V4 were cloned as previously described (Reilly et al., 2003; Sabnis et al., 2008; Deering-Rice et al., 2011). Sequence verified plasmid DNA was transfected into HEK-293 cells grown to confluence in 96-well culture dishes pre-coated for 2h with 1% gelatin using 175 ng/well plasmid DNA and Lipofectamine 2000 (Invitrogen) at a 2:1 lipid to DNA ratio in 50 μ L OptiMem media (Invitrogen) for 4h upon which 100 μ L DMEM:F12 media containing 5% Fetal Bovine Serum was added for an additional 20h. The media was replaced and cells were assayed 24h later or selected for stable over-expression by diluting and culturing in media containing 400 μ g/mL Geneticin. TRPA1, C4 α , V2, V3, V4, and M8 stable over-expressing cells were generated in our laboratory as previously described (Deering-Rice et al., 2011) while TRPM2 over-expressing cells were provided by Dr. Yasuo Mori (Kyoto University, Kyoto, Japan). TRPV1 and the TRPM8 Δ 1-801 variant were transiently over-expressed in HEK-293 using the methods described above, and TRPV1 was stably over-expressed in BEAS-2B cells as previously described (Reilly et al., 2003). Site-directed mutagenesis of TRPV1 was performed using the QuickChange XL kit (Stratagene, La Jolla, CA) and mutants were compared to wild-type receptors using transient over-expression in HEK-293 cells with normalization of data using nonivamide (25 μ M) as the agonist.

Fluorometric Calcium Flux Assays: Cells are sub-cultured into 96 well plates, grown to confluence and loaded with a membrane permeable fluorogenic Ca⁺⁺ indicator, Fluo 4-AM, using the Fluo-4 Direct Calcium Assay kit (Invitrogen). TRPV1 over-expressing BEAS-2B cells were loaded for 60 min at room temperature, while HEK-293 cells were loaded at 37°C, according to the manufacturer protocol. After loading, cells were washed once and incubated in the dark for

an additional 15-30 minutes in LHC-9 media fortified with 0.75 mM water soluble probenecid (Invitrogen) and 0.75 mM trypan red (AAT Bioquest, Sunnyvale, CA). Changes in cellular fluorescence in response to treatments (ΔF) were assessed microscopically at room temperature ($\sim 23^{\circ}\text{C}$) as previously detailed (Deering-Rice et al., 2011). Briefly, cells were treated with soluble agonists or insoluble particle suspensions by applying a 3X concentrate to achieve the final concentrations listed in the figure legends. Fluorescence images were collected at time=0 and at 30 s intervals for 3 min. The average value for change in fluorescence at each time point was determined using an image analysis program and these values were corrected for background and were further normalized to the maximum attainable response elicited by treatment of the cells with ionomycin ($10\mu\text{M}$). In some instances these data were further normalized to the response elicited by the prototypical TRP channel agonist. For clarity, the reader is reminded that the final PM concentration listed for each figure represents the concentration of the suspension of particles in the treatment well, not the actual dose at the cell surface which varies over the course of the 3 min treatment as a result of particle settling. Data in the figures represents the change in fluorescence (ΔF) measured between time=0 and 3 min.

Cell Surface TRPV1 Enrichment, Cell Surface Protein Isolation, and Immunoblotting: Pre-treatment of TRPV1-OE cells for 24h with the TRPV1 antagonist LJO-328 at $5\mu\text{M}$, as previously described (Johansen et al., 2006), was used to enrich TRPV1 at the cell surface to determine if CFA1 preferentially activated TRPV1 at the cell surface, as suggested by prior studies of TRPV1-PM interactions (Oortgiesen et al., 2000; Veronesi et al., 2002; Agopyan et al., 2003a; Agopyan et al., 2003b; Veronesi et al., 2003; Agopyan et al., 2004), or if CFA1 uptake or CFA1-derived materials released into the treatment media were the agonists. Cell surface proteins were isolated from two confluent T-75 flasks of cells/group using the Pierce Sulfo-

NHS-SS-Biotin Cell Surface Protein Isolation kit (Pierce, Rockford, IL), as instructed by the manufacturer protocol. Protein concentration was determined using the Bicinchoninic Acid Assay kit (Pierce) and equal quantities of protein from control and LJO-328 pre-treated cells were resolved by electrophoresis on a 10% NuPAGE gel (Invitrogen) and subsequently transferred to PVDF for detection of TRPV1. The membranes were blocked for 24h using 5% (w/v) dry milk and 2.5% goat serum in PBS buffer containing 0.1% v/v Tween 20 (PBS-T), then probed using a polyclonal rabbit-anti-TRPV1 antibody raised against amino acid residues 7-21 of human TRPV1 (TDLGAAADPLQKDTTC) (ab3487; Abcam, Cambridge, MA) diluted 1:2000 in blocking buffer. The membranes were washed 2X with PBS-T and probed overnight at 4°C with a goat-anti-rabbit HRP-conjugated secondary antibody (ab6721; Abcam) diluted 1:2000 in blocking buffer. After washing an additional 2X with PBS-T, the membrane were developed using the Pierce ECL Plus chemiluminescent reagent (Pierce). Relative band intensities were compared using a BioRad GelDoc Image analysis system.

PCR Analysis of Gene Expression in Human Cells: Cells were sub-cultured into 6-well (TRPV1-OE) or 12-well (NHBE) cell culture plates, grown to ~90% density, and treated for 4h (TRPV1-OE) or 24h (NHBE) at 37°C. Total RNA was extracted from cells using the Qiagen RNeasy mini kit (Qiagen, Valencia, CA) and 2.5 µg of the total RNA was converted to cDNA using Superscript III (Invitrogen). The resulting cDNA was either assayed for gene expression using multiplex PCR followed by agarose gel electrophoresis and gel densitometry, as previously described (Reilly et al., 2003; Reilly et al., 2005; Johansen et al., 2006), or diluted 1:50 for analysis by quantitative real-time PCR (qPCR). qPCR was performed using LightCycler® 480 SYBR Green I Master Mix (Roche, Indianapolis, IN) with a LightCycler® 480 System. The PCR program consisted of 10 min incubation at 95°C, followed by 40 cycles of 95°C for 15s,

55°C for 30s, then 72°C for 30s. Experiments were performed in triplicate with a copy number standard curve for both the normalization gene (β 2 macroglobulin, β 2M) and the genes of interest (GADD153, IL-6 and IL-8). Primer sequences were (5'→3'): h β 2M sense GATGAGTATGCCTGCCGTGTG and antisense CAATCCAAATGCGGCATCT; hGADD153 sense AGAACCAGGAAACGGAAACAGA and antisense TCTCCTTCATGCGCTGCTTT; hIL-6 sense AACCTGAACCTTCCAAAGATGG and antisense TCTGGCTTGTTCCCTCACTACT; hIL-8 sense ACTGAGAGTGATTGAGAGTGGAC and antisense AACCTCTGCACCCACTTTTC.

PM Instillation: Animals were maintained at the University of Utah vivarium. Food and water were available *ad libitum*. All experiments were approved by the University of Utah Institutional Animal Care and Use Committee, in accordance with the National Institutes of Health Guide for the Care and Use of Laboratory Animals. Mice (CF1 (Charles River, Wilmington, MA), C57BL/6 (Jackson Laboratories, Bar Harbor, MA), and TRPV1^{-/-} (Jackson Laboratories, Bar Harbor, MA) weighing ~20-25 g were anesthetized using ketamine (50 mg/kg) + xylazine (10 mg/kg i.p.) and suspended vertically at ~30°-45° angle on an immobilizer. The larynx was visualized by gently grasping tongue with tweezers and inserting an otoscope into the mouth; treatment solutions were slowly dispensed into the tracheal opening. Mice were instilled with 25 μ L sterile phosphate-buffered saline (PBS), nonivamide (0.5 mg/mL in 4% ethanol), or a suspension of 10 mg/mL CFA1 in sterile PBS (250 μ g total PM or ~10mg/kg). Mice were maintained in the elevated position for ~2 min after instillation and returned to their cages for 4h, upon which they were terminally anesthetized by i.p. injection of pentobarbital (100 mg/kg) and exsanguinated via the abdominal aorta. The lungs and trachea were accessed and processed for gene expression by qPCR and qualitative histological analysis. Notably, the 250 μ g i.t. dose

used in this study substantially higher than what occurs through most acute environmental exposures, but it is within the range used previously for i.t. instillations of DEP, CFA1-like materials, and other PM materials (Ogugbuaja et al., 2001; Ernst et al., 2002; Takano et al., 2002a; Takano et al., 2002b; Gilmour et al., 2004; Yokota et al., 2008; Costa et al., 2010) and could approximate a total daily dose under some circumstances. Regardless, this exposure should allow a general assessment of whether TRPV1 plays an integral role in mediating select toxicologically relevant outcomes in the mouse lung or not.

Gene Expression Analysis in Mouse Lung Tissue: Lungs were accessed and inflated with ~300 μ L RNALater solution (Ambion, Austin, TX) using a syringe. The trachea was tied closed and the trachea, bronchi, and lungs were removed and placed in RNALater at 4°C overnight and subsequently stored at -80°C. Total RNA was isolated using the Trizol-Plus Total RNA isolation kit (Invitrogen) and converted to cDNA using the Superscript III cDNA synthesis kit (Invitrogen). Quantitative PCR was performed using 2.5 μ L cDNA (diluted 1:50) in RT² SYBR Green qPCR Master Mix (SA Biosciences, Frederick MD), a Roche LightCycler® 480 instrument, and a PCR program used consisting of 10 min incubation at 95°C, followed by 40 cycles of 95°C for 15s and 63°C for 60s. Copy number standards were used for all genes. Clara Cell Specific Protein (CCSP) and Surfactant Protein-A (SPA) expression was used to confirm enrichment of bronchioles and alveolar in dissected tissue and Glyceraldehyde Phosphate Dehydrogenase (GAPDH) was used to normalize expression data. Primers were (5'→3'):

mCCSP sense ATGAAGATCGCCATCACAATCAC and antisense GGATGCCACATAACCAGACTCT; mSP-A sense GAGGAGCTTCAGACTGCACTC and antisense AGACTTTATCCCCCACTGACAG; mTRPV1 sense CATCTTCACCACGGCTGCTTAC and antisense CAGACAGGATCTCTCCAGTGAC;

mGADD153 sense GAACGAGCGGAAAGTGGCA and antisense
CATGCCGGTTCGATCAGAGCC; mGAPDH sense AGGTCGGTGTGAACGGATTTG and
antisense TGTAGACCATGTAGTTGAGGTCA; mCXCL1/KC sense
CTGGGATTCACCTCAAGAACATC and antisense CAGGGTCAAGGCAAGCCTC;
mCXCL2/MIP-2 α sense CCAACCACCAGGCTACAGG and antisense
GCGTCACACTCAAGCTCTG; and mouse IL-6 sense TAGTCCTTCCTACCCCAATTTC
and antisense TTGGTCCTTAGCCACTCCTTC.

Histology: Lungs were accessed and the trachea was cannulated with a blunt-ended needle and the lungs were inflated 10% neutral-buffered formalin at ~20 cm fixed pressure. The lungs were fixed for ~5 min, the trachea tied off, and the entire respiratory tract removed and placed in 10% neutral buffered formalin. Cross sections (~4-5 mm thick) from the bronchial insertion point to the lower portion of the left lobe were taken and used to prepare serial 5 μ m sections for staining with Hematoxylin and Eosin. Tissue sectioning and staining was performed by ARUP Laboratories (Salt Lake City, UT).

Airway Segmentation: Male CF1 mice were treated i.t. with nonivamide (0.5 mg/kg; PBS containing 4% v/v ethanol) or CFA1 (250 μ g), and the respiratory tissue was inflated with RNALater, collected as described above, and stored at 4°C. Within 48h, the lungs were dissected in a bath of RNALater and the trachea, main bronchi, bronchioles from the main bronchus (generation 3) into the parenchyma (as far as possible), and alveolar regions were collected from the left lobe. Whole lung samples were the right cranial and middle lobes. Tissues were stored at -80°C until mRNA isolation using the Trizol-Plus kit (Invitrogen), as described above. Prior to PCR analysis, mRNA from these samples was amplified. Briefly, total RNA (1 μ g) was amplified using the Message Amp II RNA amplification kit (Ambion, Austin,

TX), and as above, aRNA (1 μ g) was converted to cDNA using the Superscript III cDNA synthesis kit (Invitrogen) and assayed for gene expression by quantitative PCR.

Results:

Identification of environmental PM agonists of TRPV1 was achieved by measuring calcium influx into HEK-293 cells transiently transfected with human TRPV1 (Figure 1A). The known TRPV1 agonist nonivamide was used as positive control, and ionomycin was used to assess maximum cell fluorescence and to normalize the results for the various treatments, as described in methods. PM treatments were applied at a concentration of 0.73 mg/ml, which in previous experiments has been shown to produce a maximum TRP-dependent response (i.e., control HEK-293 cells did not exhibit a response). CFA1 produced a significant increase in calcium in TRPV1 expressing HEK-293 cells that was ~4-fold that observed in the control HEK-293 cells. DEP, as previously reported (Deering-Rice et al., 2011), and MUS also exhibited weak agonist activity, but the responses were not statistically significant. CFA2, DD, and nSiO₂ did not activate TRPV1.

The selectivity of CFA1 for TRPV1 was evaluated by assessing calcium flux in control HEK-293 cells versus HEK-293 cells transfected to over-express TRPA1, C4 α , M2, M8, the TRPM8 Δ ₁₋₈₀₁ variant, V2, V3, or V4. Quantitative results for calcium flux elicited by the various channel-specific positive controls and CFA1 are shown in Figure 1B. CFA1 was an agonist for human TRPV1, M8, and to a lesser extent A1, a result previously described for TRPA1 (Deering-Rice et al., 2011). Activation of TRPV1 by CFA1 produced a response $54 \pm 7\%$ that of the prototype agonist nonivamide, a response $47 \pm 16\%$ the prototype TRPM8 agonist icilin, and $18 \pm 5\%$ the prototype TRPA1 agonist AITC. Activation of TRPC4 α , M2, and V2-4 by CFA1 was not observed.

The mechanism of TRPV1 activation by CFA1 was pursued further due to its robust response relative to nonivamide and the postulated role of TRPV1 in mediating respiratory injury by PM. The nature of the agonist responsible for CFA1-induced calcium flux (i.e., extracellular vs. intracellular CFA1 or insoluble vs. soluble CFA1 components) was compared in TRPV1-OE cells, with, and without, LJO-328 pre-treatment to increase the cell surface abundance of TRPV1 (Johansen et al., 2006). LJO-328 pre-treated cells exhibited an approximate 6-fold increase in immunoreactive TRPV1 protein on the cell surface and were ~5-fold more responsive to CFA1 than non-pretreated cells (Figure 2A and B). CFA1-induced calcium flux in the LJO-328 pre-treated TRPV1-OE cells was inhibited by co-treating cells with CFA1 and the TRPV1 antagonist LJO-328, as well as the non-selective cell surface calcium channel blocking agents EGTA and ruthenium red (Figure 2B). Manipulation of CFA1 by washing and solvent extraction was also used to illustrate that the solid components of CFA1 were the agonist of TRPV1. CFA1 recovered following overnight incubation and repeated (3X) washing with LHC-9 elicited a response that was $117 \pm 19\%$ that of CFA1 freshly suspended in LHC-9 ($100 \pm 23\%$) ($p > 0.05$) and the clarified overnight media extract did not have agonist activity. Likewise, CFA1 washed 3X1h with 1 mL 1:1 chloroform:methanol, elicited a response that was $82 \pm 12\%$ that of fresh CFA1 ($p > 0.05$), with no response observed for the dried and reconstituted organic extract residues. Of note, the residue did contain trace quantities of insoluble CFA1 material indicating the reduction in CFA1 potency observed by organic extraction may have been due to particle loss, and not partial removal of a soluble agonist.

The mechanism of TRPV1 activation by CFA1 was interrogated using site-directed mutagenesis of known functionally important amino acid residues of TRPV1 to identify key particle-protein interactions governing activity (Figure 3A and B). Mutation of Y511 (Y511A),

an intramembrane residue required for TRPV1 activation by capsaicinoids (Jordt and Julius, 2002; Bessac and Jordt, 2008) did not have a negative effect on CFA1 activity. Similarly, mutation of the proton potentiation site (Jordt et al., 2000), E649 (E649A) increased the CFA1 response ~2-fold relative to wild type TRPV1. Mutation of C578 (C578A), the voltage- and cation-sensitive residue E600 (E600V) (Jordt et al., 2000; Ahern et al., 2005), and the glycosylation site N604 (N604A) (Wirkner et al., 2005), and the double mutants C578A+E600V and C578A+N604A all exhibited a diminished response to CFA1, but mutation of the redox sensitive residue C621 (C621A) (Jin et al., 2004) and agonist/antagonist peptide binding residues A658 (A658P) and F660 (F660A) (Bohlen et al., 2010; Lin et al., 2011), had no effect on TRPV1 activation by CFA1.

The role of TRPV1 in mediating pro-apoptotic and immunomodulatory cytokine/chemokine production by lung cells treated with CFA1, a response previously shown for other TRPV1-activating PM and other TRPV1 agonists (Veronesi et al., 1999a; Veronesi et al., 1999b; Oortgiesen et al., 2000; Agopyan et al., 2003b; Thomas et al., 2007; Thomas et al., 2011), was evaluated (Figure 4). Treatment of NHBE cells with CFA1 increased the expression of mRNA for the pro-apoptotic gene product GADD153 (3-fold control), the cytokine IL-6 (18-fold control), and the chemokine IL-8 (22-fold control) (Figure 4A), which were suppressed 82, 73, and 87%, respectively, by LJO-328 co-treatment. In TRPV1-OE cells, induction of IL-6 and IL-8 mRNA, relative to mRNA for β -actin, was also exacerbated by LJO-328 pre-treatment (Figure 4B), consistent with cell surface TRPV1 acting as the gene product responsible for translating CFA1 contact with the cell surface to changes in the expression of these pro-inflammatory genes.

In addition to the cell culture studies, the role of CFA1 in activating TRPV1 was assessed in an animal model. The induction of pro-apoptotic and pro-inflammatory responses in the intact mouse lung and airway tissue was assessed using intratracheal administration of nonivamide and CFA1. CF-1 mice were instilled intratracheally with nonivamide (Figure 5A) or CFA1 (Figure 5B) and the respiratory tissue was assayed for regional changes in GADD153, CXCL-1/KC, CXCL-2/MIP-2 α , and IL-6 mRNA expression, relative to control values obtained from PBS-instilled mice; CXCL-1/KC and CXCL-2/MIP-2 α constitute the functional equivalents of human IL-8. Significant induction of CXCL-1/KC, CXCL-2/MIP-2 α , and IL-6 were generally observed in whole lung and bronchiole tissue 4h following nonivamide (Figure 5A) and CFA1 (Figure 5B) treatment, compared to PBS instilled controls. Decreased expression of GADD153 was observed in the trachea, and to a lesser extent, in the bronchi of nonivamide- and CFA1-treated mice, as previously reported for nonivamide (Thomas et al., 2011), and CXCL-1/KC was elevated in alveolar tissue, however, these responses were not statistically significant. Histological analysis of lung tissue from CFA1-treated mice demonstrated CFA1 was retained in the bronchioles and alveoli (Figure 6), consistent with the gene expression data in Figure 5B; no such material was observed in PBS- or nonivamide-treated mice (data not shown).

Finally, CFA1-induced changes in GADD153, CXCL-1/KC, CXCL-2/MIP-2 α , and IL-6 were compared in wild-type C57BL/6 and TRPV1^{-/-} C57BL/6 mice (Figure 7). No changes in GADD153 expression were detected, but significant increases in CXCL-1/KC, CXCL-2/MIP-2 α , and IL-6 were observed in lungs of wild-type mice. CFA1-induced expression of CXCL-1/KC, CXCL-2/MIP-2 α , and IL-6 was reduced in TRPV1^{-/-} mice, but statistical significance was only achieved for CXCL-2/MIP-2 α .

Discussion:

This study investigated the hypothesis that TRPV1 is differentially activated by chemically and physically unique PM and that activation of TRPV1 by a PM agonist in lung cells and the respiratory tract would promote changes in the expression of pro-inflammatory and ER-stress associated genes that may contribute to pulmonary injury by inhaled PM. It is shown that TRPV1 is activated by some (CFA1, DEP, MUS), but not all PM; TRPM8 is also robustly activated by CFA1, and TRPA1 is slightly activated; activation of TRPV1 by CFA1 occurs via cell surface interactions between the solid components of CFA1 and specific amino acid residues of TRPV1 localized to the putative pore-loop region; and activation of TRPV1 by CFA1 is not exclusive in mouse lungs, but represents a pathway by which CFA1 impacts the expression of selected genes in lung epithelial cells and airway tissue.

Previous studies characterizing the activation of TRPV1 in lung cells by PM were limited in that they did not directly evaluate potential contributions of other calcium channels, despite evidence that ASIC channels also contributed to the responses (Veronesi et al., 1999a; Veronesi et al., 1999b; Oortgiesen et al., 2000; Veronesi et al., 2002; Agopyan et al., 2003a; Agopyan et al., 2003b; Veronesi et al., 2003; Wong et al., 2003; Ghelfi et al., 2008). Bronchial epithelial and airway sensory neurons cells express numerous other TRP channels that also could be activated by different forms of PM. For example, TRPA1 and TRPM8 are expressed by airway vagal and trigeminal sensory neurons that respond to PM, and TRPA1 is largely co-expressed with TRPV1 while TRPM8 is expressed independent of TRPA1 and V1 (Kobayashi et al., 2005). Similarly, TRPM8 exists as a functional variant, TRPM8 $_{\Delta 1-801}$ (Sabnis et al., 2008), in lung epithelial cells which also express high levels of TRPV4 (Li et al., 2011) which may also contribute to lung cell responses to certain forms of PM. Figures 1, 2 and 4 substantiate previous conclusions that

TRPV1 mediates the induction of several important pro-apoptotic and pro-inflammatory cytokine/chemokine genes in lung epithelial cells to in response to PM. However, while near complete inhibition of CFA1-induced calcium flux and gene expression changes were achieved using LJO-328 co-treatment of lung epithelial cells (Figures 2B and 4A), as shown by others using capsaizepine and other forms of PM, only partial attenuation of gene induction was observed in TRPV1^{-/-} mice relative to wild-type mice (Figure 7). These results, in conjunction with Figure 1B, suggest a possible role for neuronal TRPA1 or TRPM8 as additional mediators of lung inflammation and toxicity elicited by CFA1. Alternatively, pathways that were not evaluated in these studies may also contribute to the effects of CFA1 in the lung, particularly at the high dose of CFA1 used, where the precise contribution of TRPV1 may be poorly estimated. Ongoing dose-response studies and future research employing more relevant exposure methods (e.g., inhalation of suspended PM for multiple days), combined with additional genetic and/or pharmacological inhibitors should provide a more complete model for TRPV1, A1, M8, and other PM sensors collectively contribute to the adverse effects of PM in the lung. Regardless, TRPV1 does play an important role in detecting CFA1 and initiating specific responses that likely contribute to the adverse effects of this and other similar PM in the respiratory tract.

Prior studies have also partially characterized the mechanism of activation of TRPV1 and demonstrated a requirement for cell surface contact and a net-negative surface charge on PM to elicit responses (Oortgiesen et al., 2000; Agopyan et al., 2003a; Agopyan et al., 2003b). In this study, it is confirmed that TRPV1 activation by CFA1 occurs as a result of interactions between CFA1 and cell surface TRPV1. First, enrichment of TRPV1 at the cell surface enhanced both CFA1-induced calcium flux (Figures 2A and B) and IL-6 and 8 mRNA expression (Figure 4B), with the latter serving as a “*reporter assay*” for cell surface TRPV1 activation, as supported by

previous studies (Reilly et al., 2005; Johansen et al., 2006). Second, chelation of calcium ions in the treatment media with EGTA, and co-treating cells with the cell-impermeable TRPV1 pore blocker ruthenium red, inhibited calcium flux comparable to that achieved using the selective cell-permeable TRPV1 antagonist LJO-328, which inhibits total cellular TRPV1 (Figure 2B). Finally, the agonist activity of CFA1 was localized to the aqueous- and solvent- (1:1 chloroform:methanol) insoluble CFA1. Thus, unlike the activation of TRPA1 by electrophiles that can be extracted by alcohol and/or solvent treatments and are released from DEP upon cell contact (Deering-Rice et al., 2011), soluble CFA1-derived components do not activate TRPV1, providing a second specific mechanism by which two unique forms of environmental PM activate two specific TRP channels in the airway.

Consistent with prior proposed mechanisms of TRPV1 activation by negatively-charged PM (Oortgiesen et al., 2000; Veronesi et al., 2002; Agopyan et al., 2003a; Agopyan et al., 2003b; Veronesi et al., 2003), and results in Figure 2 and 3B, it was demonstrated that mutation of the capsaicin binding site residue Y511 (Y511A), located on the intracellular loop between transmembrane segments 3 and 4, did not reduce TRPV1 activation by CFA1, despite completely inhibiting the response to nonivamide. Conversely, neutralization of the cell surface pore-loop residue E649 (E649A), which is predicted to reside at the entry to the ion pore domain at the membrane surface, forming a “base” of a cylindrical tetrameric pore region (Figure 3A), increased TRPV1 activation by CFA1 ~2-fold, relative to wild-type TRPV1. One interpretation of this result is that interactions between the pore-loop segment of TRPV1 (roughly residues 600-660), specifically E600, N604 (and/or the N-linked glycan attached at this position) (Wirkner et al., 2005) are facilitated as a result of a reduction in charge-charge repulsive forces that may occur between E649 and CFA1 (Figure 3A). However, this scenario does not fully

explain the apparent roles for C578, E600, and N604 in CFA1-mediated activation of TRPV1. As such, from the collective data in Figure 3, reports that TRPV1, like other TRP channels, can be activated by mechanical mechanisms (Inoue et al., 2009), and identification of a sequence of the extracellular pore loop residues that displaces upon thermal activation (Yang et al., 2010), it is proposed that C578, E600, and N604 may be components of a “*charge- and mechanosensitive*” domain. Thus, the following model is proposed (refer to Figure 3A for a visual aid): 1) extracellular components of TRPV1 form a “*basket-like structure*” above the ion pore opening; 2) E600, and N604 reside at the membrane interface potentially constituting a flexible “*hinge region*” that must be displaced in order for CFA1 to activate TRPV1, and the presence of N604-linked glycans facilitate this process; 3) the base of the “*basket-like structure*” interacts with CFA1 in a charge-dependent manner and neutralization of E649 leads to increased interaction by negatively-charged PM; and 4) mechanical movement of the cell surface “*turret*” or “*basket wall*” components of TRPV1 are transduced into pore opening through interactions between C578 and yet undefined residues of the pore domain.

In summary, this study further illustrates that TRPV1 detects and differentially responds to select forms of environmental PM, and that TRPV1 activation contributes to several commonly cited cellular responses to PM including pro-apoptotic and pro-inflammatory gene induction in lung cells and airway tissue. It is anticipated that further elucidation of the contributions of TRPV1 and/or other related TRP channels to PM effects in the respiratory tract will reveal novel therapeutic opportunities to prevent and/or attenuate such effects in humans.

Author Contributions:

Participated in research design: Deering-Rice, Johansen, Yost, Veranth, Reilly

Conducted experiments: Deering-Rice, Johansen, Roberts, Romero, Thomas, Reilly

Contributed new reagents: Lee

Performed data analysis: Deering-Rice, Romero, Roberts, Reilly

Wrote or contributed to writing of the manuscript: Deering-Rice, Veranth, Yost, Reilly

References:

- Agopyan N, Bhatti T, Yu S and Simon SA (2003a) Vanilloid receptor activation by 2- and 10-micron particles induces responses leading to apoptosis in human airway epithelial cells. *Toxicol Appl Pharmacol* **192**:21-35.
- Agopyan N, Head J, Yu S and Simon SA (2004) TRPV1 receptors mediate particulate matter-induced apoptosis. *Am J Physiol Lung Cell Mol Physiol* **286**:L563-572.
- Agopyan N, Li L, Yu S and Simon SA (2003b) Negatively charged 2- and 10-microm particles activate vanilloid receptors, increase cAMP, and induce cytokine release. *Toxicol Appl Pharmacol* **186**:63-76.
- Ahern GP, Brooks IM, Miyares RL and Wang XB (2005) Extracellular cations sensitize and gate capsaicin receptor TRPV1 modulating pain signaling. *J Neurosci* **25**:5109-5116.
- Bernstein JA, Alexis N, Barnes C, Bernstein IL, Nel A, Peden D, Diaz-Sanchez D, Tarlo SM and Williams PB (2004) Health effects of air pollution. *J Allergy Clin Immunol* **114**:1116-1123.
- Bessac BF and Jordt SE (2008) Breathtaking TRP channels: TRPA1 and TRPV1 in airway chemosensation and reflex control. *Physiology (Bethesda)* **23**:360-370.
- Bohlen CJ, Priel A, Zhou S, King D, Siemens J and Julius D (2010) A bivalent tarantula toxin activates the capsaicin receptor, TRPV1, by targeting the outer pore domain. *Cell* **141**:834-845.
- Cao X, Xu X, Cui W and Xi Z (2001) Development and certification of a coal fly ash certified reference material for selected polycyclic aromatic hydrocarbons. *Fresenius J Anal Chem* **370**:1035-1040.

- Chow JC, Watson JG, Mauderly JL, Costa DL, Wyzga RE, Vedal S, Hidy GM, Altshuler SL, Marrack D, Heuss JM, Wolff GT, Pope CA, 3rd and Dockery DW (2006) Health effects of fine particulate air pollution: lines that connect. *J Air Waste Manag Assoc* **56**:1368-1380.
- Costa SK, Kumagai Y, Brain SD, Teixeira SA, Varriano AA, Barreto MA, de Lima WT, Antunes E and Muscara MN (2010) Involvement of sensory nerves and TRPV1 receptors in the rat airway inflammatory response to two environment pollutants: diesel exhaust particles (DEP) and 1,2-naphthoquinone (1,2-NQ). *Arch Toxicol* **84**:109-117.
- Deering-Rice CE, Romero EG, Shapiro D, Hughen RW, Light AR, Yost GS, Veranth JM and Reilly CA (2011) Electrophilic Components of Diesel Exhaust Particles (DEP) Activate Transient Receptor Potential Ankyrin-1 (TRPA1): A Probable Mechanism of Acute Pulmonary Toxicity for DEP. *Chem Res Toxicol* **24**:950-959.
- Ernst H, Rittinghausen S, Bartsch W, Creutzenberg O, Dasenbrock C, Gorlitz BD, Hecht M, Kairies U, Muhle H, Muller M, Heinrich U and Pott F (2002) Pulmonary inflammation in rats after intratracheal instillation of quartz, amorphous SiO₂, carbon black, and coal dust and the influence of poly-2-vinylpyridine-N-oxide (PVNO). *Exp Toxicol Pathol* **54**:109-126.
- Fernandez-Ballester G and Ferrer-Montiel A (2008) Molecular modeling of the full-length human TRPV1 channel in closed and desensitized states. *J Membr Biol* **223**:161-172.
- Ghelfi E, Rhoden CR, Wellenius GA, Lawrence J and Gonzalez-Flecha B (2008) Cardiac oxidative stress and electrophysiological changes in rats exposed to concentrated ambient particles are mediated by TRP-dependent pulmonary reflexes. *Toxicol Sci* **102**:328-336.

- Gilmour MI, O'Connor S, Dick CA, Miller CA and Linak WP (2004) Differential pulmonary inflammation and in vitro cytotoxicity of size-fractionated fly ash particles from pulverized coal combustion. *J Air Waste Manag Assoc* **54**:286-295.
- Glinianaia SV, Rankin J, Bell R, Pless-Mulloli T and Howel D (2004) Particulate air pollution and fetal health: a systematic review of the epidemiologic evidence. *Epidemiology* **15**:36-45.
- Inoue R, Jian Z and Kawarabayashi Y (2009) Mechanosensitive TRP channels in cardiovascular pathophysiology. *Pharmacol Ther* **123**:371-385.
- Jia Y, McLeod RL and Hey JA (2005) TRPV1 receptor: a target for the treatment of pain, cough, airway disease and urinary incontinence. *Drug News Perspect* **18**:165-171.
- Jin Y, Kim DK, Khil LY, Oh U, Kim J and Kwak J (2004) Thimerosal decreases TRPV1 activity by oxidation of extracellular sulfhydryl residues. *Neurosci Lett* **369**:250-255.
- Johansen ME, Reilly CA and Yost GS (2006) TRPV1 antagonists elevate cell surface populations of receptor protein and exacerbate TRPV1-mediated toxicities in human lung epithelial cells. *Toxicol Sci* **89**:278-286.
- Jordt SE and Julius D (2002) Molecular basis for species-specific sensitivity to "hot" chili peppers. *Cell* **108**:421-430.
- Jordt SE, Tominaga M and Julius D (2000) Acid potentiation of the capsaicin receptor determined by a key extracellular site. *Proc Natl Acad Sci U S A* **97**:8134-8139.
- Kobayashi K, Fukuoka T, Obata K, Yamanaka H, Dai Y, Tokunaga A and Noguchi K (2005) Distinct expression of TRPM8, TRPA1, and TRPV1 mRNAs in rat primary afferent neurons with adelta/c-fibers and colocalization with trk receptors. *J Comp Neurol* **493**:596-606.

- Li J, Kanju P, Patterson M, Chew WL, Cho SH, Gilmour I, Oliver T, Yasuda R, Ghio A, Simon SA and Liedtke W (2011) TRPV4-Mediated Calcium-influx into Human Bronchial Epithelia upon Exposure to Diesel Exhaust Particles. *Environ Health Perspect*.
- Lighty JS, Veranth JM and Sarofim AF (2000) Combustion aerosols: factors governing their size and composition and implications to human health. *J Air Waste Manag Assoc* **50**:1565-1618; discussion 1619-1522.
- Lin Z, Reilly CA, Antemano R, Huguen RW, Marett L, Concepcion GP, Haygood MG, Olivera BM, Light A and Schmidt EW (2011) Nobilamides A-H, Long-Acting Transient Receptor Potential Vanilloid-1 (TRPV1) Antagonists from Mollusk-Associated Bacteria. *J Med Chem* **54**:3746-3755.
- Ogugbuaja VO, Onyeyili PA and Moses EA (2001) Study of effects on haematological parameters of rabbits intratracheally exposed to coal fly ash. *J Environ Sci Health A Tox Hazard Subst Environ Eng* **36**:1411-1418.
- Oortgiesen M, Veronesi B, Eichenbaum G, Kiser PF and Simon SA (2000) Residual oil fly ash and charged polymers activate epithelial cells and nociceptive sensory neurons. *Am J Physiol Lung Cell Mol Physiol* **278**:L683-695.
- Pope CA, 3rd, Renlund DG, Kfoury AG, May HT and Horne BD (2008) Relation of heart failure hospitalization to exposure to fine particulate air pollution. *Am J Cardiol* **102**:1230-1234.
- Reilly CA (2010) Neurogenic Inflammation: The Role of TRP Channels in the Lung. , in *Comprehensive Toxicology 2nd edition* (McQueen CA ed), Elsevier.
- Reilly CA, Johansen ME, Lanza DL, Lee J, Lim JO and Yost GS (2005) Calcium-dependent and independent mechanisms of capsaicin receptor (TRPV1)-mediated cytokine production and cell death in human bronchial epithelial cells. *J Biochem Mol Toxicol* **19**:266-275.

- Reilly CA, Taylor JL, Lanza DL, Carr BA, Crouch DJ and Yost GS (2003) Capsaicinoids cause inflammation and epithelial cell death through activation of vanilloid receptors. *Toxicol Sci* **73**:170-181.
- Sabnis AS, Shadid M, Yost GS and Reilly CA (2008) Human lung epithelial cells express a functional cold-sensing TRPM8 variant. *Am J Respir Cell Mol Biol* **39**:466-474.
- Smith KR, Veranth JM, Kodavanti UP, Aust AE and Pinkerton KE (2006) Acute pulmonary and systemic effects of inhaled coal fly ash in rats: comparison to ambient environmental particles. *Toxicol Sci* **93**:390-399.
- Takano H, Yanagisawa R, Ichinose T, Sadakane K, Inoue K, Yoshida S, Takeda K, Yoshino S, Yoshikawa T and Morita M (2002a) Lung expression of cytochrome P450 1A1 as a possible biomarker of exposure to diesel exhaust particles. *Arch Toxicol* **76**:146-151.
- Takano H, Yanagisawa R, Ichinose T, Sadakane K, Yoshino S, Yoshikawa T and Morita M (2002b) Diesel exhaust particles enhance lung injury related to bacterial endotoxin through expression of proinflammatory cytokines, chemokines, and intercellular adhesion molecule-1. *Am J Respir Crit Care Med* **165**:1329-1335.
- Thomas KC, Roberts JK, Deering-Rice CE, Romero EG, Dull RO, Lee J, Yost GS and Reilly CA (2011) Contributions of TRPV1, Endovanilloids, and Endoplasmic Reticulum Stress in Lung Cell Death In Vitro and Lung Injury. *Am J Physiol Lung Cell Mol Physiol*.
- Thomas KC, Sabnis AS, Johansen ME, Lanza DL, Moos PJ, Yost GS and Reilly CA (2007) Transient receptor potential vanilloid 1 agonists cause endoplasmic reticulum stress and cell death in human lung cells. *J Pharmacol Exp Ther* **321**:830-838.

- Veranth JM, Cutler NS, Kaser EG, Reilly CA and Yost GS (2008) Effects of cell type and culture media on Interleukin-6 secretion in response to environmental particles. *Toxicol In Vitro* **22**:498-509.
- Veranth JM, Moss TA, Chow JC, Labban R, Nichols WK, Walton JC, Watson JG and Yost GS (2006) Correlation of in vitro cytokine responses with the chemical composition of soil-derived particulate matter. *Environ Health Perspect* **114**:341-349.
- Veranth JM, Reilly CA, Veranth MM, Moss TA, Langelier CR, Lanza DL and Yost GS (2004) Inflammatory cytokines and cell death in BEAS-2B lung cells treated with soil dust, lipopolysaccharide, and surface-modified particles. *Toxicol Sci* **82**:88-96.
- Veronesi B, Carter JD, Devlin RB, Simon SA and Oortgiesen M (1999a) Neuropeptides and capsaicin stimulate the release of inflammatory cytokines in a human bronchial epithelial cell line. *Neuropeptides* **33**:447-456.
- Veronesi B, de Haar C, Lee L and Oortgiesen M (2002) The surface charge of visible particulate matter predicts biological activation in human bronchial epithelial cells. *Toxicol Appl Pharmacol* **178**:144-154.
- Veronesi B, Oortgiesen M, Carter JD and Devlin RB (1999b) Particulate matter initiates inflammatory cytokine release by activation of capsaicin and acid receptors in a human bronchial epithelial cell line. *Toxicol Appl Pharmacol* **154**:106-115.
- Veronesi B, Wei G, Zeng JQ and Oortgiesen M (2003) Electrostatic charge activates inflammatory vanilloid (VR1) receptors. *Neurotoxicology* **24**:463-473.
- Ward DJ and Ayres JG (2004) Particulate air pollution and panel studies in children: a systematic review. *Occup Environ Med* **61**:e13.

- Wirkner K, Hognestad H, Jahnel R, Hucho F and Illes P (2005) Characterization of rat transient receptor potential vanilloid 1 receptors lacking the N-glycosylation site N604. *Neuroreport* **16**:997-1001.
- Wong SS, Sun NN, Keith I, Kweon CB, Foster DE, Schauer JJ and Witten ML (2003) Tachykinin substance P signaling involved in diesel exhaust-induced bronchopulmonary neurogenic inflammation in rats. *Arch Toxicol* **77**:638-650.
- Yang F, Cui Y, Wang K and Zheng J (2010) Thermosensitive TRP channel pore turret is part of the temperature activation pathway. *Proc Natl Acad Sci U S A* **107**:7083-7088.
- Yokota S, Ohara N and Kobayashi T (2008) The effects of organic extract of diesel exhaust particles on ischemia/reperfusion-related arrhythmia and on pulmonary inflammation. *J Toxicol Sci* **33**:1-10.

Footnotes:

This work was supported by grants from the National Institutes of Health National Institute of Environmental Health Sciences [ES017431], and the 2011 Colgate-Palmolive Postdoctoral Fellowship awarded to Cassandra E. Deering-Rice. Development and synthesis of LJO-328 was supported by the National Research Foundation of Korea [R11-2007-107-02001-0] awarded to Jeewoo Lee.

Figure Legends:

Figure 1: (A) Nonivamide, CFA1, MUS, and DEP activate TRPV1 and cause calcium influx (ΔF) into TRPV1-expressing HEK-293 cells (grey bars) versus control HEK-293 cells (white bars). Nonivamide (Noniv.; positive control for TRPV1) was applied at 25 μM for 1 min and PM was applied at 0.73 mg/mL for 3 min. Data are the mean and SEM ($n \geq 3$) for ΔF relative to ionomycin (10 μM) and asterisks indicate a statistical difference between control HEK-293 cells and TRPV1-overexpressing HEK-293 cells when treated with PM using 2-way ANOVA and post-testing using the Bonferroni multiple comparisons test. (B) CFA1 activates TRPV1, TRPM8 and TRPA1. HEK-293 cells transiently (TRPV1 and TRPM8 $_{\Delta 1-801}$), or stably (all others), over-expressing human TRP channels were treated with a prototype agonist for the specific receptor (white bars) or CFA1 at 0.73 mg/mL for 3 min (grey bars). The prototype agonists were used at a concentration determined to yield a maximum receptor-specific response and were: TRPA1 (AITC; 150 μM); TRPC4 α (carbachol; 0.75 μM); TRPM2 (H₂O₂; 1 mM); TRPM8 (icilin; 50 μM); TRPM8 $_{\Delta 1-801}$ (-menthol; 2500 μM); TRPV1 (nonivamide; 25 μM); TRPV2 (THC; 100 μM); TRPV3 (carvacrol; 250 μM); and TRPV4 (GSK1016790A; 0.0125 μM). Data are the mean and SEM ($n \geq 3$) for ΔF relative to ionomycin (10 μM) and asterisks indicate a statistically significant response in overexpressing cells versus HEK-293 cells treated with either a prototypical receptor agonist or CFA1 using 2-way ANOVA and post-testing using the Bonferroni multiple comparisons test. ** $p < 0.01$, *** $p < 0.001$, N.D. = no response detected.

Figure 2: (A) Pre-treatment of TRPV1-OE BEAS-2B cells with LJO-328 (5 μM ; 24h) stimulates cell surface expression of TRPV1 and CFA1-induced calcium flux. Top panel: Increased recovery and detection of TRPV1 in cell surface protein isolates of LJO-328 pre-treated TRPV1-

OE (right lane) versus non-pretreated TRPV1-OE cells (left lane) by western blot. Bottom panel: Images showing calcium flux in TRPV1-OE cells treated with LHC-9 media (negative control; left), 0.73 mg/mL CFA1 for 3 min (center), or LJO-pretreated cells (right) treated with 0.73 mg/mL CFA1 for 3 min. Bright green spots represent fluorescent cells where TRPV1-mediated calcium flux was observed. **(B)** Quantitation of calcium flux in TRPV1-OE cells treated with CFA1, with or without, LJO-328 pre-treatment and inhibition of calcium flux by total (LJO-328) or cell-impermeable and non-selective (EGTA and Ruthenium Red) TRPV1 inhibitors. The white bars represent calcium flux in normal TRPV1-OE cells treated with LHC-9 (negative control) or CFA1 at 0.73 mg/mL for 3 min, the light grey bars are LJO-328 pre-treated TRPV1-OE cells treated with either LHC-9 or CFA1 at 0.18 or 0.73 mg/mL for 3 min, and the black bars are LJO-328 pre-treated TRPV1-OE cells co-treated with CFA1 at 0.73 mg/mL for 3 min and either EGTA+Ruthenium Red (50 + 250 μ M) or LJO-328 (20 μ M). Data are the mean and SEM (n=5) and asterisks indicate a statistical difference relative to the media control, or response to CFA1 between non-pretreated and LJO-328 pretreated cells. Daggers indicate a significant reduction in response between LJO-328 pre-treated cells treated with CFA1, with and without inhibitor co-treatment using 1-way ANOVA with post-testing using the Bonferroni multiple comparisons test. **** $p < 0.0001$, ††† $p < 0.0001$.

Figure 3: **(A)** Annotated homology model (Fernandez-Ballester and Ferrer-Montiel, 2008) of a TRPV1 subunit outside and inside the cell membrane (upper images), the TRPV1 tetramer viewed from the outside in (lower left image), and two TRPV1 subunits (lower right image), highlighting residues effecting TRPV1 activation by CFA1. **(B)** Quantitative calcium flux results showing that pore-loop residues of TRPV1 regulate responses to CFA1. The images in

Figure 3A and Figure 3B are color-coded where green represents stimulatory point mutations and red for inhibitory point or double mutants. Data are the mean and SEM ($n \geq 5$) and asterisks indicate a statistical difference relative to wild-type TRPV1 using ANOVA with Dunnett's multiple comparison post-test. $*p < 0.05$, $**p < 0.01$, $***p < 0.001$.

Figure 4: (A) CFA1-induced changes in GADD153, IL-6, and IL-8 mRNA in NHBE cells following 24h treatment at 37°C with 0.23 mg/mL CFA1. Control (white bars), CFA1 (grey bars), and CFA1 plus LJO-328 (20 μ M) co-treatment (black bars). Data are the mean and SEM ($n=3$) and asterisks indicate a statistical increase in mRNA abundance relative to untreated control cells while daggers indicate a decrease in mRNA induction with LJO-328 co-treatment using 2-way ANOVA with a Bonferroni multiple comparisons post-test. (B) Image of PCR-amplified DNA for IL-6, IL-8 and β -actin DNA in an ethidium bromide-stained 2% agarose gel. cDNA was prepared from TRPV1-OE cells treated with LHC-9 (negative control; left lane), 0.43 mg/mL CFA1 (center lane), and LJO-328 pre-treated TRPV1-OE cells treated with CFA1 (0.43 mg/mL) for 4h at 37°C. $**p < 0.01$, $***p < 0.001$, $^\dagger p < 0.01$, $^\dagger\dagger p < 0.001$.

Figure 5: Quantification of GADD153, CXCL-1/KC, CXCL-2/MIP-2 α , and IL-6 mRNA, relative to GAPDH mRNA, in CF-1 mouse respiratory tissues by quantitative real-time PCR, 4h following intratracheal administration of (A) nonivamide (0.5 mg/kg) or (B) CFA1 (250 μ g). Data are the mean and SEM ($n \geq 3$) and asterisks indicate statistical significance relative to PBS-treated mice using 2-way ANOVA with a Bonferroni multiple comparisons post-test. $*p < 0.05$, $**p < 0.01$, $***p < 0.001$

Figure 6: Mouse lung histology. Sections of mouse lung were assessed at 160X to localize CFA1 (brown/black materials) retained in the lung 4h post i.t. treatment with PM (250 µg). Images are characteristic of results from the analysis of CFA1-treated mouse lungs and there was no evidence of such materials in lungs of PBS- or nonivamide-treated mice (images not shown).

Figure 7: Quantification of GADD153, CXCL-1/KC, CXCL-2/MIP-2 α , and IL-6 mRNA, relative to GAPDH mRNA, in wild-type C57BL/6 (white bars) and TRPV1^{-/-} C57BL/6 (grey bars) mouse lung tissue assayed by quantitative real-time PCR, 4h following intratracheal administration of CFA1 (250 µg). Data are the mean and SEM (n \geq 6). Asterisks indicate statistical significance relative to PBS-treated controls and daggers indicate a statistical decrease in expression in TRPV1^{-/-} mice relative to wild-type mice using 2-way ANOVA with the Bonferroni multiple comparisons post-test. * $p < 0.05$, ** $p < 0.01$, $\dagger\dagger p < 0.01$, $\dagger p < 0.05$.

Figure 1:

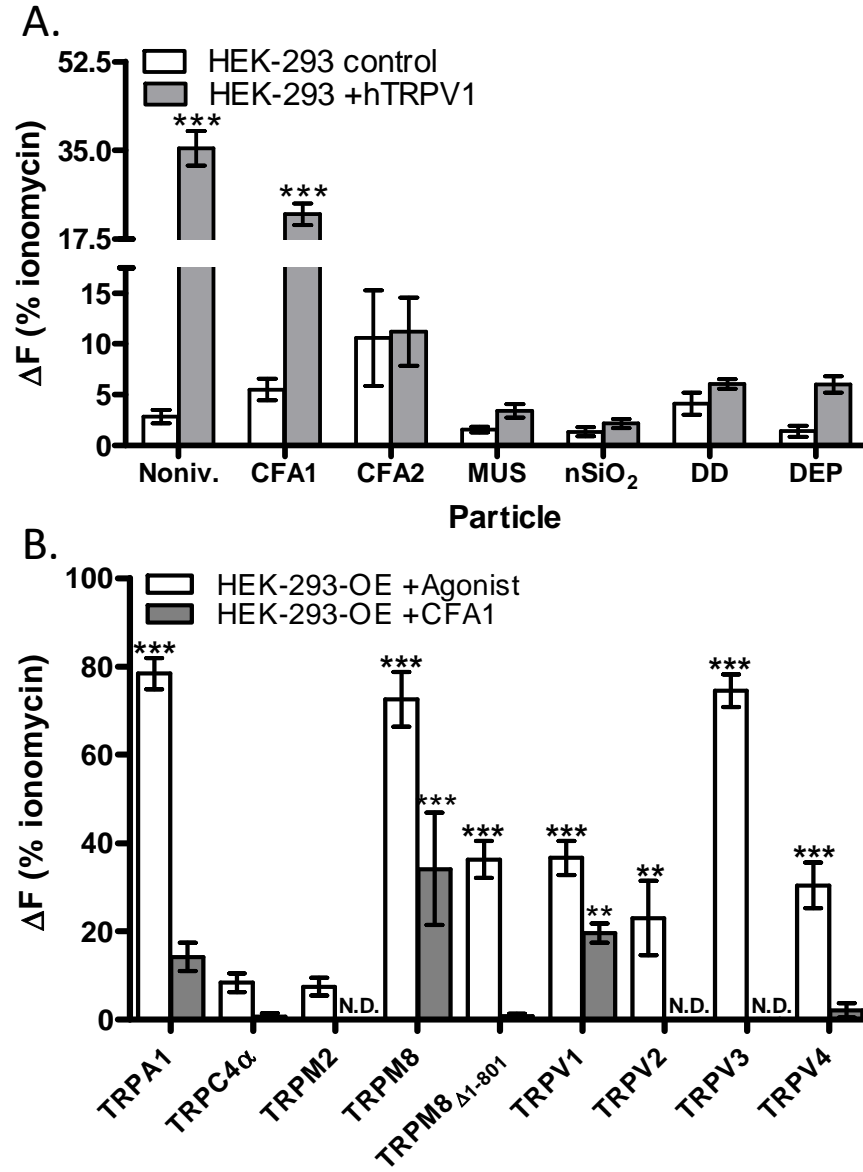


Figure 2:

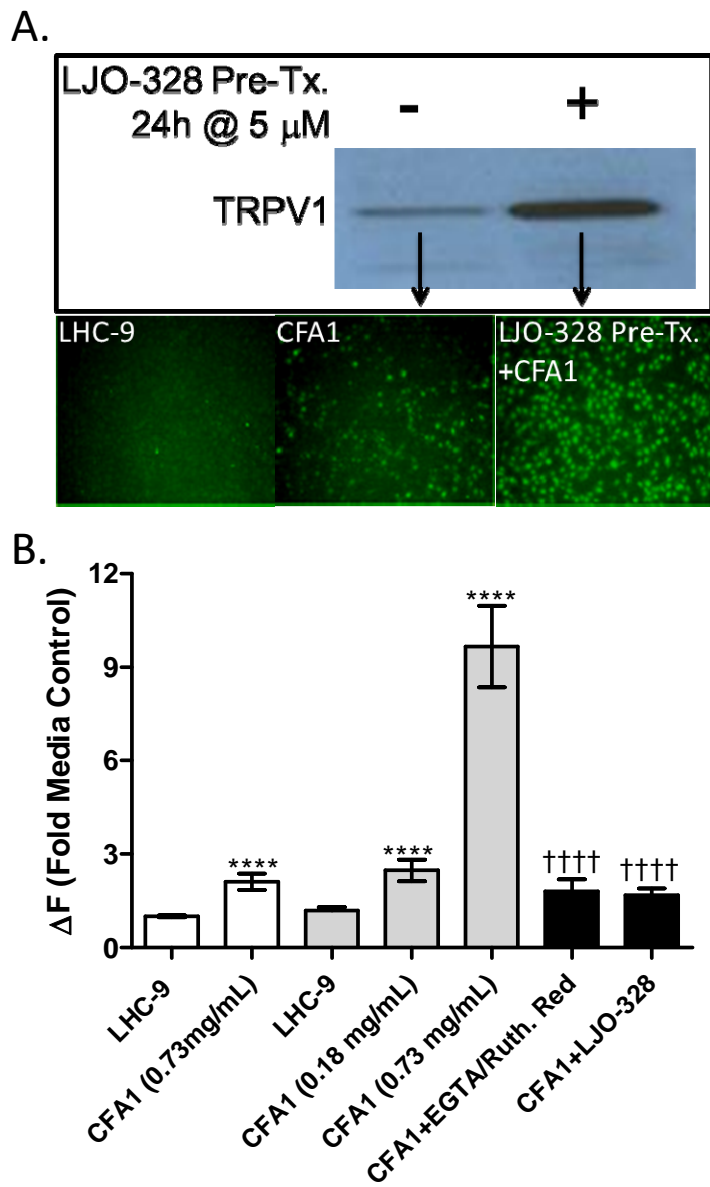


Figure 3:

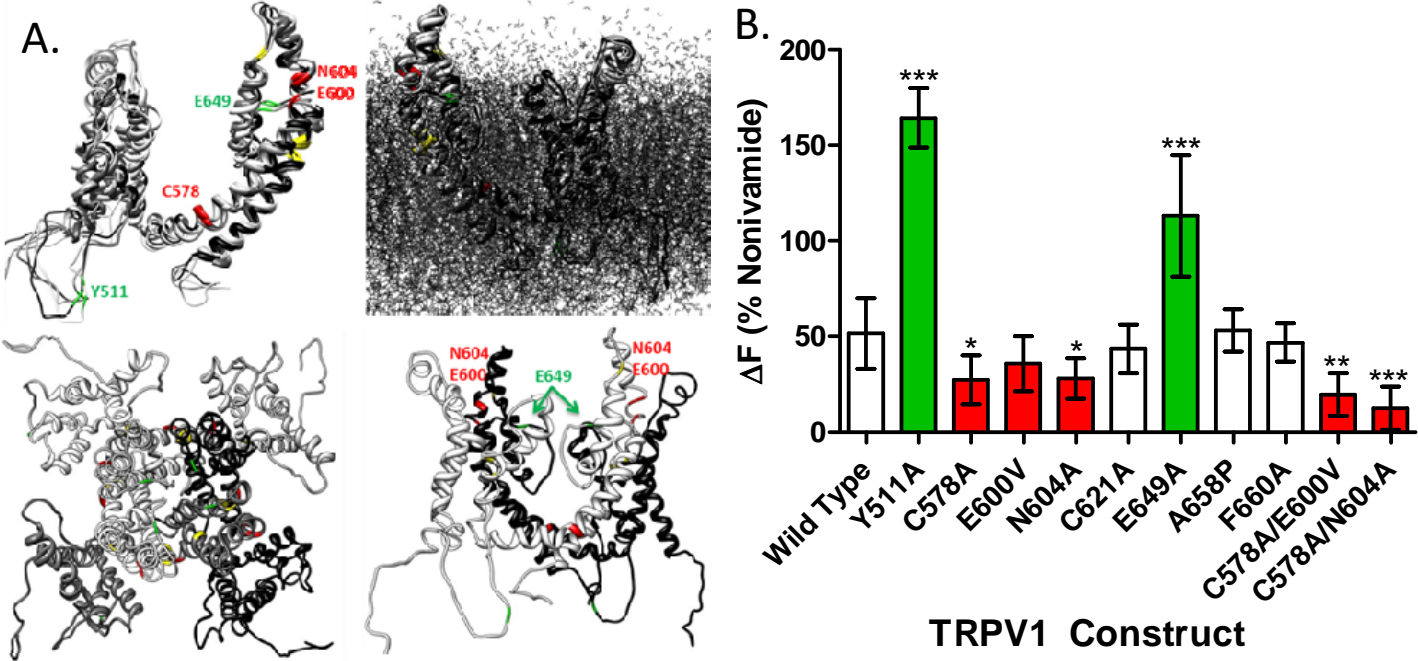


Figure 4:

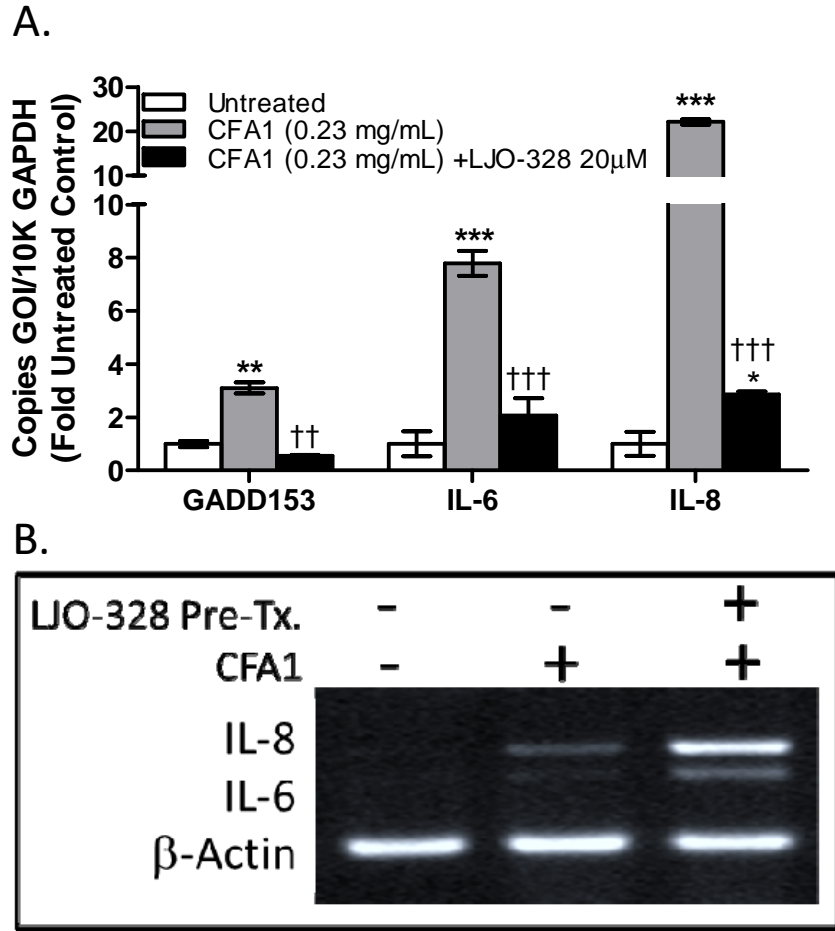
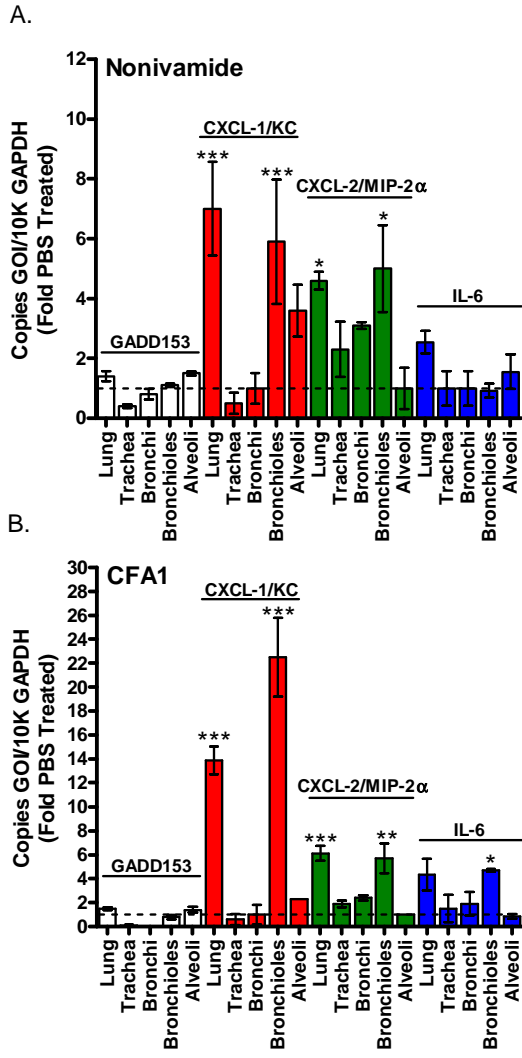


Figure 5:



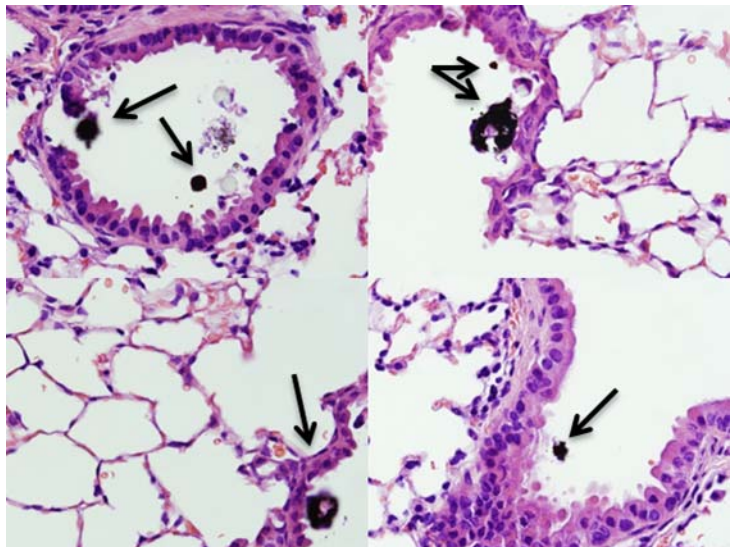


Figure 6:

Figure 7:

